WIDEBAND SUBHARMONICALLY PUMPED W-BAND MIXER IN SINGLE-RIDGE FIN-LINE*

L-2

Paul J. Meier

Eaton Corporation
AIL Division
Melville, New York

Summary

A subharmonic mixer is described with an instantaneous bandwidth of 12 GHz centered near 95 GHz. The wide bandwidth is achieved by closely integrating a low-capacitance diode mount, printed-circuit matching elements, and simple yet effective filters which are uniquely suited to realization in single-ridge fin-line.

Introduction

Subharmonically pumped mixers have been constructed in various transmission media including stripline[1], microstrip, waveguide[2] and double-ridged fin-line[3]. Although excellent results have been obtained at millimeter wavelengths[4], tunable waveguide backshorts have so far limited the instantaneous bandwidth. This paper describes a subharmonic mixer with an instantaneous bandwidth of 12 GHz centered near 95 GHz. The wide bandwidth is achieved by closely integrating a low-capacitance diode mount with printed-circuit matching elements and simple, yet effective, filters which are uniquely suited to realization in single-ridge fin-line. The following paragraphs describe the design and performance of the subject mixer.

Circuit Description

Figure 1 shows the construction features of the wideband single-ridge fin-line mixer. The fin-line is printed on 5-mil Duroid which is suspended in the E-plane of a rectangular housing. The housing has the same inner dimensions as WR-10 waveguide, in the indicated region. The gap (d) between the edge of the fin and the upper housing wall is chosen to be small enough to propagate the subharmonic local oscillator (LO), and yet large enough to accommodate the antiparallel diodes. By selecting a gap ratio (d/b) equal to 0.3, the cutoff frequency of the fin-line is placed at 37 GHz, which is well below the intended LO band.

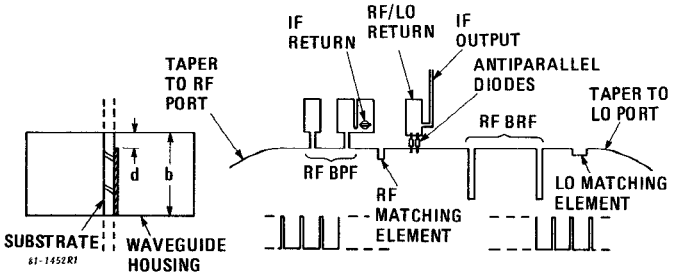

Figure 1. Subharmonic Mixer in Single-Ridge Fin-Line

The RF signal enters from the left and passes through a cosine taper which matches the fin-line to a standard WR-10 port. The signal then passes through a single-section band-pass filter (BPF). The filter is formed by two inductive strips, each joining the edge of the fin to a ground return. Grounding in the RF and LO bands is achieved with low-impedance stubs within the choke region[5] of the housing. Grounding in the IF band is provided by a feedthrough which links the illustrated pattern to a rear-surface metallization. After exiting from the BPF, the signal passes through the RF matching element and reaches the antiparallel diodes which are reactively terminated by the RF band-reject filter (BRF). The diodes are mounted between the edge of the fin and a low-impedance stub which is the RF/LO ground return. The IF leaves the low-capacitance diode mount through a microstrip line and an SMA connector (not shown).

The LO enters the circuit from the right in Figure 1. The LO-matching elements include a notch in the fin-line, a cosine taper and a step in the width of the housing. The latter allows the subharmonic pump to propagate without the aid of the fin-line, and it also provides a direct interface with a standard WR-19 port. After emerging from the matching elements, the LO passes through the RF band-reject filter and reaches the diode mount, which is reactively terminated by the RF band-pass filter.

The fin-line filters which diplex the RF and LO are key components of the subject mixer. The analysis, design, and performance of these filters are discussed next.

Equivalent Circuits for Filters

The fin-line filters were analyzed and optimized by computer-aided techniques, based on the equivalent circuits shown in Figure 2. The circuit for the band-pass filter (Figure 2A) includes the normalized shunt susceptances (b_3 and b_5) separated by a line length (ℓ_4) which controls the resonant frequency. The circuit also includes input and output lines (ℓ_2 and ℓ_6) which model the dissipative loss in the cosine tapers. All the transmission lines are assigned a normalized characteristic impedance of unity (that is, the tapers are assumed to be reflectionless).

The magnitude of the shunt susceptance was determined by embedding a single inductive strip between matched transitions and measuring the insertion loss across the bands of interest (40 to 60 GHz and 80 to 110 GHz). At each frequency, the normalized susceptance was calculated from:

$$b = 2\sqrt{\log^{-1}(L/10) - 1}$$

where L is the measured loss (less the transition loss) in dB. After investigating a variety of analytical expressions, it was demonstrated that the susceptance could be accurately modeled by the equation:

*The work reported was partially funded by NOSC under Contract Number N00123-79-C-1879

$$b = k(f - f_c)^n$$

where f and f_c are the operating and cutoff frequencies, respectively. The constants k and n were determined to be 181 and -1.27, respectively, based on a log/log plot of b versus $f - f_c$. Because of this exponential variation, the susceptance is an order of magnitude larger in the LO band than it is in the RF band. This condition is highly favorable to the design of the RF band-pass filter. The exponential variation assures that high rejection in the LO band and a wide RF bandwidth can be simultaneously obtained with a simple one-section filter.

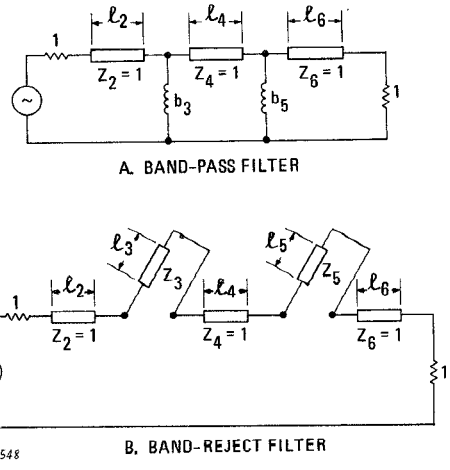

Figure 2. Equivalent Circuits of Fin-Line Filters

Figure 2B shows the equivalent circuit of the RF band-reject filter, which is utilized at the LO port of the mixer. The filter consists of two notches which are etched into the fin-line. It has been shown that such a structure can be modeled by shortcircuited stubs, appearing in a series with the main line[6]. The circuit contains the series lines (ℓ_3 and ℓ_5) which are each a quarter-wave long at the center of the rejection band. The stubs are spaced along the main line by ℓ_4, the length that controls the match in the desired passband, as well as the center frequency of the second passband. (The latter falls above the rejection band at a frequency where ℓ_4 is approximately a half wavelength.) The equivalent circuit also includes input and output lines (ℓ_2 and ℓ_6) to model dissipative loss in the cosine tapers.

Filter Design and Performance

Through a computer-aided analysis of the circuit of Figure 2A, a suitable resonator length (ℓ_4) was chosen for the RF band-pass filter. Based on the assumption that the electrical and mechanical values of ℓ_4 were equal, a breadboard model of the RF band-pass filter was constructed and tested. The measurements showed that the passband was centered at a frequency 7-percent higher than that desired. Using this information, the design was refined to include an offset between ℓ_4 and the centerline spacing of the inductive strips. Figure 3 shows the measured performance of the revised RF filter, together with the calculated response. The measured rejection is better than 25 dB in the LO band of 42 to 51 GHz and the insertion loss is 1.4 $\pm$0.4 dB across the RF band of 86 to 102 GHz. The loss, measured from flange to flange in an oversized fixture, includes superfluous line lengths which were eliminated in the subharmonic mixer. The RF input loss in the final mixer design is estimated to be 0.5 dB.

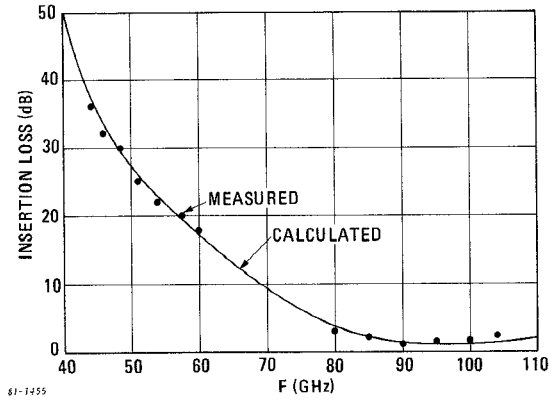

Figure 3. Response of RF Band-Pass Filter

It should be emphasized that the favorable asymmetric response of Figure 3 was obtained with a single-section fin-line filter. To duplicate this performance with quasi-lumped elements in a TEM medium, at least six elements would be required.

The RF band-reject filter was designed with the aid of the equivalent circuit of Figure 2B. Based on published information[6], plausible magnitudes were assigned to z_3 and z_5, and the remaining variables (ℓ_3 through ℓ_5) were optimized by computer-aided calculations. After obtaining a satisfactory response, a breadboard filter was constructed and tested. The model was then refined to obtain the best fit with the measurements. Good agreement was obtained with:

$z_3 = z_5 = 0.95$

ℓ_4 = physical spacing between the slots

$\ell_3 = \ell_5$: 17% longer than the physical slot length

With these parameters, the computer model was utilized to optimize the filter performance for the intended application. Calculations showed that ℓ_4 should be a half wavelength just above the stop band. This prevents a spurious response within the RF band and yet keeps ℓ_4 as large as possible, thereby obtaining a favorable (quarter wave) spacing of the slots near the LO band. Figure 4 compares the measured and calculated response of the optimized band-reject filter. The half-wave response has been fixed at 108 GHz, which provides ample rejection at the upper edge of the RF band. Across the RF band of 86 to 102 GHz, the measured and calculated rejection is greater than 20 dB. In the LO band, the measured insertion loss, from flange to flange, is typically 1 dB. Since the measurement includes superfluous line lengths and a pair of WR-19/WR-10 transitions, the LO input loss in the final mixer is estimated to be 0.5 dB.

Mixer Integration and Performance

The previously described filters were next integrated with antiparallel diodes and other circuit elements to form a mixer similar to that shown in Figure 1. In the first phase of integration, however, the circuit did not include RF- or LO-matching elements. In keeping with the wideband objective, low-parasitic

beam-lead devices[7] were chosen for the antiparallel diodes. The RF band-pass filter was located a quarter LO wavelength from the diodes to provide a wideband back-short termination. The band-reject filter, which appears as an open-circuit to the RF, was located as close to the diodes as possible. The LO- and RF-matching elements were then added, respectively, and optimized by an iterative technique.

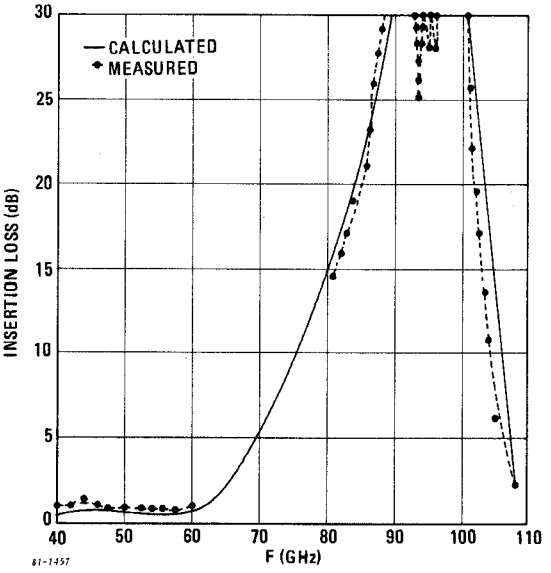

Figure 4. Response of Two-Slot BRF

Figure 5 shows the measured conversion loss of a preliminary model of the integrated mixer, with an LO drive level of 16 dBm. The conversion loss is plotted versus the signal frequency, with the LO frequency as a parameter. With the LO fixed at 45 GHz, the conversion loss is 12 ±2 dB across a 12-GHz band centered at 95.5 GHz. When the LO is increased by 1 GHz, the IF increases by 2 GHz and the ripple, in the upper portion of the band, shifts accordingly. This suggests that the ripple is due to IF mismatch in the band above 5 GHz. It is believed that better flatness could be achieved, with further work, by improving the IF match.

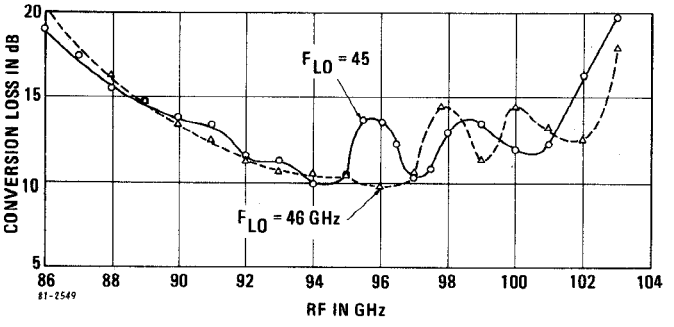

Figure 5. Conversion Loss of Mixer

Figure 6 shows the conversion loss of the preliminary mixer versus LO power, for typical RF and LO frequencies. With the LO fixed at 46 GHz, 13 dBm is adequate for optimum performance. At 45 GHz, however, the minimum conversion loss is achieved with a drive level of 16 dBm. This agrees with the measured LO-port return loss.

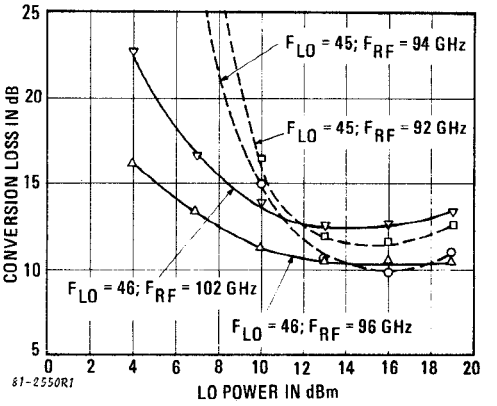

Figure 6. Conversion Loss vs LO Power

Conclusions

A subharmonically pumped mixer has been developed with an unprecedented useful instantaneous bandwidth of 12 GHz centered near 95 GHz. The wide bandwidth is achieved by closely integrating a low-capacitance diode mount, printed-circuit matching elements, and simple yet effective filters which are uniquely suited to realization in single-ridge fin-line. A minimum conversion loss of 10 dB has been obtained and calculations[8] show that a 2-dB improvement is possible. The current limitation is attributed to unequal diode bonding inductance[9] and the finite separation between the diodes. Both effects can be reduced by replacing the two diodes with a single antiparallel device[7] now under development.

Acknowledgments

The work reported was partially funded by NOSC under the direction of J. E. Reindel. The work was performed at Eaton Corporation AIL Division under the direction of B. J. Peyton and J. J. Whelehan. The diodes were developed by J. A. Calviello and P. R. Bie under the direction of J. J. Taub. Technical assistance was provided by A. Cooley, A. Kunze, J. Pieper and A. Rees.

References

1. M. V. Schneider and W. W. Snell, IEEE Trans. Vol. MTT-23, pp. 271-275, March 1975.

2. M. Cohn, J. E. Degenford and B. A. Newman, IEEE Trans. Vol. MTT-23, pp. 667-673, August 1975.

3. G. Begemann, Digest of IEEE 1981 MTT-S Symposium, pp. 454-456, June 1981.

4. E. R. Carlson, M. V. Schneider and T. T. McMaster, IEEE Trans. Vol. MTT-26, pp. 706-715, October 1978.

5. P. J. Meier, IEEE Trans. Vol. MTT-26, pp. 726-733, October 1978.

6. H. Hofmann, Digest of IEEE 1980 MTT-S Symposium, pp. 59-61, May 1980.

7. J. A. Calviello, S. Nussbaum and P. R. Bie, Digest of IEEE International Electron Devices Meeting, pp. 692-695, December 1981.

8. E. W. Sard, Private Communication, November 1981.

9. R. G. Hicks and P. J. Khan, Digest of IEEE 1981 MTT-S Symposium, pp. 457-459, June 1981.